Testing excision techniques for dynamical 3D black hole evolutions

Miguel Alcubierre,[1] Bernd Brügmann,[2] Peter Diener,[3,4]
Frank Herrmann,[5] Denis Pollney,[5] Ed Seidel,[3,4,5] and Ryoji Takahashi[4]

[1]*Instituto de Ciencias Nucleares, Universidad Nacional Autónoma de México, A.P. 70-543, México D.F. 04510, México.*
[2]*Institute for Gravitational Physics and Geometry, Penn State University, University Park, PA 16802, U.S.A.*
[3]*Department of Physics and Astronomy, Louisiana State University, Baton Rouge, LA 70803, USA*
[4]*Center for Computation and Technology, 302 Johnston Hall, Louisiana State University, Baton Rouge, LA 70803, USA*
[5]*Max Planck Institut für Gravitationsphysik, Albert Einstein Institut, Am Muehlenberg 1, 14476 Golm, Germany*

(Dated: February 7, 2008)

We perform both distorted black hole evolutions and binary black hole head on collisions and compare the results of using a full grid to results obtained by excising the black hole interiors. In both cases the evolutions are found to run essentially indefinitely, and produce the same, convergent waveforms. Further, since both the distorted black holes and the head-on collision of puncture initial data can be carried out without excision, they provide an excellent dynamical test-bed for excision codes. This provides a strong numerical demonstration of the validity of the excision idea, namely the event horizon can be made to "protect" the spacetime from the excision boundary and allow an accurate exterior evolution.

PACS numbers: 04.25.Dm, 04.30.Db, 95.30.Sf, 97.60.Lf
Preprint number: IGPG-04/10-5, AEI-2004-114

arXiv:gr-qc/0411137v1 29 Nov 2004

I. INTRODUCTION

A successful numerical model of a binary black hole collision will require the refinement of a number of specialized techniques. A particular problem of black hole simulations is handling the strong fields in the neighborhood of the physical singularity. The method of "singularity excision" promises to solve, or rather avoid, this difficulty. Black hole excision was first discussed by Thornburg [1, 2, 3] based on a suggestion by Unruh [4]. Within the event horizon of a spacetime all light-cones corresponding to the flow of physical information in the fields point "inwards". Thus a boundary within the event horizon forms a one way membrane, with information flowing only into the hole. Physical data on such a boundary should not influence the external spacetime. In a numerical simulation, this implies that errors on the boundary, for instance due to extrapolations from the exterior, should not be expected to propagate to the exterior spacetime. However, because of the complicated and nonlinear nature of the equations being solved, complex relationships link the finite differenced evolution equations to artificial boundary conditions. It is often the case that the full implications of using a particular technique are poorly understood, and can only be judged by some amount of experimentation.

The excision idea has a long history of implementations in numerical relativity codes in 1D, 2D and 3D. The basic concept was developed into a set of techniques for practical application in 1D in [5], where causal differencing techniques and dynamical lapse and shift conditions designed for excision were introduced and shown to increase stability and accuracy of dynamic BH spacetimes (coupled to self-gravitating scalar fields) by orders of magnitude. This work was extended both to 3D BH evolutions [6] and to a large class of shift conditions in [7] such as the geometrically motivated distance freezing, area freezing, expansion freezing and minimal distortion shift. These ideas were later applied to more complex spacetimes, e.g. [8, 9, 10, 11, 12, 13, 14], typically using the Arnowitt-Deser-Misner (ADM) evolution system and analytic shift conditions.

With the switch to the more stable BSSN evolution system [15, 16, 17, 18, 19] and the accompanying improvements in stability of 3D codes, the excision idea was revisited by Alcubierre and Brügmann in the form of an algorithm which they called "Simple Excision" [20, 21]. The idea was to attempt an implementation which removed some complications that had hindered previous efforts, namely causal differencing within the horizon, and complicated interpolations onto an irregular boundary. Instead, the excision region was fixed as a cubical region with faces along constant Cartesian coordinate planes, simplifying the determination of a normal, and a simple source-term-copy boundary condition replaced true causal differencing. The result proved to be remarkably successful at evolving distorted single black hole spacetimes allowing accurate evolutions of unlimited length in time.

More recently advances in excision in 3D Cartesian coordinates have been reported, using different techniques, for scalar fields in fixed black hole backgrounds [22, 23] (see also [24]) and for evolutions of single black hole spacetimes [13, 25, 26]. In general, the excision problem becomes much better controlled when using coordinates that are adapted to the excision surface, and furthermore when using hyperbolic formulations and making use of the characteristic information about the propagation of

all degrees of freedom. Spherical excision is used in spectral codes [27, 28, 29] but has also been proposed for finite difference codes using multi-patch techniques [30, 31, 32].

A basic premise of the excision method is that the excision boundary data should not propagate to the exterior spacetime. In practice, it is important to verify that this is in fact the case for a given numerical implementation, and to quantify any errors that might be introduced. In this paper, we propose to compare long term black hole evolutions using singularity excision to corresponding evolutions carried out over a full grid, but with otherwise identical initial data and evolution methods. A useful excision method should yield essentially identical evolutions, and thus identical physical measurements, in the region of the spacetime outside of the horizon.

The main candidates for evolution without excision are methods using singularity avoiding slicings, where the gauge condition on the lapse slows evolution of the hypersurface in regions where a physical black hole singularity is approached. In fact, singularity avoiding slicing conditions (for example, maximal slicing or algebraic lapse conditions of the "1+log" family) were the method of choice in most simulations prior to the development of excision techniques. Without appropriate shift conditions, slice stretching arises due to the differential infall of coordinates, severely limiting the evolution time. It has only very recently been shown that an appropriately chosen shift vector can alleviate these problems, so that they occur at a much later time (or even not at all for a fixed resolution) and the final black hole settles to its expected stationary state [33, 34].

For this reason, comparisons between evolutions with and without excision are rarely done. Even worse, in most cases where excision has been successfully used, very crude measures, such as "time to crash", or some overall measure of the Hamiltonian constraint have been used as a measure of success. With the exception of a small number of results [11, 21], it has generally not been verified that, for example, correct gravitational waveforms can be extracted with excision, a point which is crucial for upcoming gravitational wave observations. As these waves will typically be very small perturbations (of order 10^{-3} or less) of the metric [35, 36, 37] very small errors generated by the excision techniques could easily swamp the signals being extracted. Furthermore, even if the excision properly preserves the causal structure, allowing no physical signals to propagate out from inside the horizon, gauge effects may well propagate to the outside, influencing the solution. This could show up not only in metric functions but also in so-called gauge-invariant waveforms, since such waveforms are only invariant under *infinitesimal* gauge transformations given some assumptions about the background coordinate system. A large gauge wave propagating through the spacetime may very well be seen in waves extracted in this way.

In this paper, we propose to use both waveforms, extracted far from the horizon, and detailed information extracted from apparent horizons just outside the excision region, as important test quantities for spacetimes evolved both with and without excision. Such tests would have been difficult or impossible in the past because, until recently, 3D BH simulations without excision became rapidly inaccurate and crashed after evolution times of only $t \approx 30 - 40 M_{ADM}$, where M_{ADM} is the ADM mass. However, the recent development of powerful shift conditions has to some extent cured the problem of slice stretching associated with singularity avoiding slicing, making it possible to evolve certain classes of distorted and colliding BH spacetimes much longer (for thousands of M_{ADM}) and much more accurately than ever before, without the need for excision [33]. This makes it possible for the first time to carry out systematic, long term studies of the effects of the excision technique on the evolved BH spacetimes.

Following Refs. [35, 36, 37, 38] we use distorted black hole initial data sets, whose waveforms can be independently and reliably computed, as testbeds for the excision techniques we use. Those papers showed that even modes with energies of order $10^{-7} M_{ADM}$ could be very accurately extracted in a full 3D numerical evolution, as confirmed by comparisons with purely perturbative evolutions. We will use some of the same testbeds proposed there in this paper.

We also apply the ideas to the study of BH collisions, using Brill-Lindquist-type initial data which, as showed in Ref. [33], can be evolved indefinitely without resorting to excision. Although Misner data have been much more extensively studied [39, 40, 41] and would be an excellent test-bed, we use Brill-Lindquist here because of their close relation to the Brill-Lindquist family of "puncture" data often applied in generating data for binary BHs in quasi-circular orbit [42, 43, 44, 45, 46]. These data sets possess apparent horizons in the initial slice, allowing excision regions to be defined, but have also been evolved for unlimited times without excision (after merger). As such, these evolutions provide an ideal test-bed for excision methods. If the excision method is valid and the exterior spacetime is protected from errors on the excision boundary by the event horizon, then simulations with excision should accurately reproduce the non-excised results. Because the testbeds we use here are highly dynamic, distorted and colliding black holes, evolved in general coordinate systems in 3D Cartesian coordinates, without resort to special conditions or tricks, successful tests of excision techniques against independently computed physics results would provide a certain amount of confidence that the techniques can be applied to more complex systems, such as orbiting black holes, where the detailed physics is more critical to get right.

In the next section we briefly outline the methods used in our black hole simulations. There follows a description of the excision region and boundary conditions which we are applying. Finally, we present numerical results in which distorted and binary black hole evolutions using excision are compared directly with those performed

without excision.

II. MODEL AND METHODS

A. Initial Data and Evolution Methods

The details of the formulation which we have implemented numerically are outlined in [33]. Briefly, we make use of the "BSSN" evolution system [15, 16, 17]. The evolution variables are a conformal factor, the conformally decomposed metric, the trace-free extrinsic curvature tensor and its trace. Additionally, the contracted conformal Christoffel symbols $\tilde{\Gamma}^i := \tilde{\gamma}^{jk}\tilde{\Gamma}^i_{jk}$ are evolved as independent variables. These variables can be regarded as gauge source functions, and in our evolutions are used to fix the shift vector through e.g. the condition $\partial_t \tilde{\Gamma}^i = 0$, which results in an elliptic shift condition analogous to minimal distortion [47]. In practice, instead of applying this elliptic shift condition directly, we use a hyperbolic "Gamma driver" version as described in Eq. (46) of [33],

$$\partial_t^2 \beta^i = F\, \partial_t \tilde{\Gamma}^i - (\eta - \frac{\partial_t F}{F})\, \partial_t \beta^i. \qquad (2.1)$$

The parameter η is a driver term which controls the growth of the shift and is discussed in more detail later, and F is a function which can be used to condition its overall shape.

The black hole initial data we use comes in two classes. The first class is the "Brill wave plus black hole" family of distorted BHs, constructed topologically as wormholes isometrically connecting two asymptotically flat spacetimes. These data sets have proved a rich and powerful system for developing many techniques in numerical relativity and for studying the physics of many aspects of distorted BHs [21, 35, 36, 37, 48, 49, 50, 51, 52, 53, 54, 55].

The second class is Brill-Lindquist binary BH initial data in isotropic coordinates [56]. The topology of these data sets is that of an asymptotically flat spacetime connected through wormholes to two disconnected asymptotically flat ends. These data sets are time symmetric and set the stage for BH head-on collisions.

As discussed in [33, 57], for spacetimes in which there is enough symmetry (such as the axisymmetric head-on collision), it is possible to carry out expansions of the evolution of the metric quantities at the "punctures" (the points in $\mathcal{R}^3$ at the "center" of each BH representing the compactified asymptotically flat regions on the other side of the wormholes), thus ensuring that the evolution variables remain regular there. By careful consideration of the evolution at the punctures, it is therefore possible to carry out long-term evolutions with the punctures included on the grid, i.e. without excision.

B. Lego Excision

The excision boundary condition which we apply is a variation of the "Simple Excision" methods described in [20]. The important difference is that instead of excising a cubical region, we excise an irregular region. The size and shape of the excision region is determined dynamically by the location of the apparent horizon. On a Cartesian grid, the resulting surface is a blocky quasi-spherical region, prompting the name "lego excision" for this method.

The update of all interior points on the grid (including those within the apparent horizon) is carried out using centered differences. That is, no causal differencing is applied. The exceptions are advection terms on the shift (terms of the form $\beta^i \partial_i$), for which a second order upwind in the shift direction is applied.

For points on the excision boundary itself, a centered update scheme cannot be used for lack of data to one side. Instead, data at these points are updated using a time derivative term which is copied from one point out. This has the effect of allowing a certain amount of evolution to take place on the boundary, while also allowing the boundary to "settle down" as the system settles to what should be a stationary end state, exemplified by $\partial_t \phi = 0$ for the fields ϕ [67]. The neighboring point from which the time derivative is copied is determined by a normal to the surface at the point. The time derivative from the point nearest to the normal is copied to the boundary point.

For the models in question, we assume that the excision region neither shrinks nor moves across the grid. In other words, it is not possible for grid points to emerge from the excision region: once excised, a point remains excised. While this may at first seem like a strong limitation, in fact even with these restrictions the technique is adequate for many binary BH inspiral studies. Under reasonable gauge choices it should be expected that the BH horizons individually should either remain of an approximately fixed coordinate size, or grow slightly, as is the case for the final post-merger BH. Further, for binary BH inspirals, co-rotating coordinates reduce the amount of dynamics on the grid to the dynamical time-scale of the problem in question, and either remove or greatly reduce the orbital motion of the individual bodies. Co-rotating coordinate systems have been proposed (see, e.g. [58]), and implemented for cases of BH binaries [59, 60, 61] (for neutron stars see e.g. [62]). For the puncture data which we have used here, the punctures are fixed to the grid. As such, problems involving movement of the excision region do not arise in these cases, almost by construction.

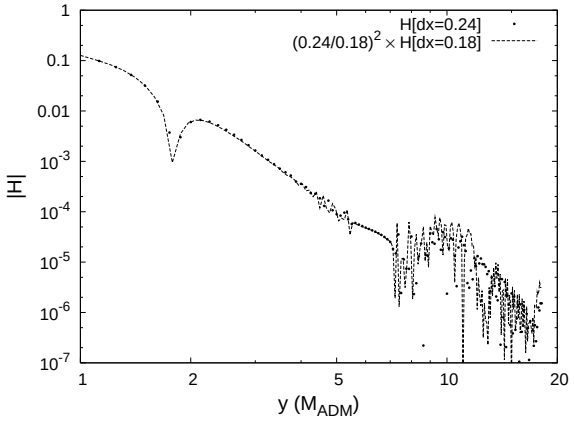

FIG. 1: The absolute value of the Hamiltonian constraint $|H|$ for a distorted black hole simulation without excision, evaluated along the y-axis at $T = 9.38M_{ADM}$ ($x = z = 0$). The high resolution Hamiltonian is scaled such that the two curves should coincide for second order convergence.

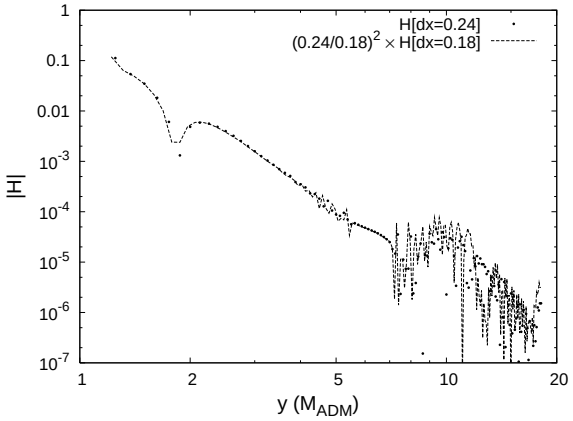

FIG. 2: Absolute value of the Hamiltonian constraint $|H|$ along the y-axis for the same distorted black hole simulation shown in Fig. 1, but this time using excision. The Hamiltonian constraint was computed at $T = 9.38M_{ADM}$.

III. APPLICATIONS

A. Results for Distorted Black Hole

As a first application we study a simulation of a distorted BH which has been studied extensively in previous work [21, 35, 36, 37, 38, 48, 49]. The BH is initially distorted by an even parity Brill wave and, for a low enough amplitude wave, during the evolution the BH rings at quasi-normal frequencies before settling down to a Schwarzschild BH. The parameters used here are, in the notation of [21, 48, 49, 63], $Q_0 = 0.1$, $\eta_0 = 0$, $\sigma = 1$. For this simulation the computational domain extends to ± 34.80 (in coordinate units). For these initial data parameters, $M_{ADM} = 1.92$, which puts the outer boundary at $\pm 18.13 M_{ADM}$. We also use two different resolutions, the smallest one with a $288 \times 288 \times 144$ sized uniform grid and a coordinate resolution of 0.24, and the largest with a $384 \times 384 \times 192$ sized uniform grid and a resolution of 0.18. An explicit reflection symmetry about the $z = 0$ plane is used.

We evolve this system both with and without excision, using identical evolution parameters. For the gauge we use a Gamma driver shift condition as specified in Eq. (2.1), and 1+log slicing. In the simulation using excision, the lego excision region was located at 80% of the apparent horizon radius, with a minimum buffer size of at least 5 grid points between the excision region and the apparent horizon surface. We find the horizon using methods described in [64, 65], and implemented as in [65]. At higher resolution the size of the buffer was adjusted such that the excision region remained at approximately the same position.

In Fig. 1 and Fig. 2 we show convergence plots for the absolute value of the Hamiltonian constraint along the y-axis at time $T = 9.38M_{ADM}$, for the runs without and with excision, respectively. In both plots the higher resolution case is scaled by a factor of $(0.24/0.18)^2$ so that, in case of second order convergence, the two curves should coincide. Note that, in both cases, we have second order convergence in the regions that are causally disconnected from the outer boundaries. In Fig. 2 points inside the excision region have been removed from the plot. Note that outside the excision region the curve is very similar to that of Fig. 1. The noise visible in both plots at $y > 7M_{ADM}$ is due to numerical details of the initial data constraint solver.

In Fig. 3 we plot the difference between the Hamiltonian constraint between runs with and without excision at $T = 9.38M_{ADM}$ at the two different resolutions, with the high resolution case again scaled as in the previous plots. Only the points outside the excision region are shown in the plot. The figure shows that there are indeed small differences between the two cases, but that these differences converge away at second order outside of the excision region.

As an indicator for analyzing excision effects we use the ratio C_r of the circumference along a polar direction in the xz-plane, to the circumference in the equatorial xy-plane, of the apparent horizon, as a function of time. As these measurements are made very close to the excision region, and as for the low amplitude Brill wave studied here C_r remains within about 1% of the Schwarzschild value of unity, we regard this as a very sensitive indicator for these tests. In Fig. 4, these ratios are plotted for evolutions with excision (lines) and without (dots) at two resolutions. The differences are very small in comparison to the size of the physical wave, and much smaller with increased of resolution. Note that in this plot the non-excision curves do not extend over the same time as the excision data. The earlier termination of the non-excision runs in Fig. 4 was due to a hardware problem and was not caused by problems in the code.

In Fig. 5 we show the evolution of the Zerilli wave

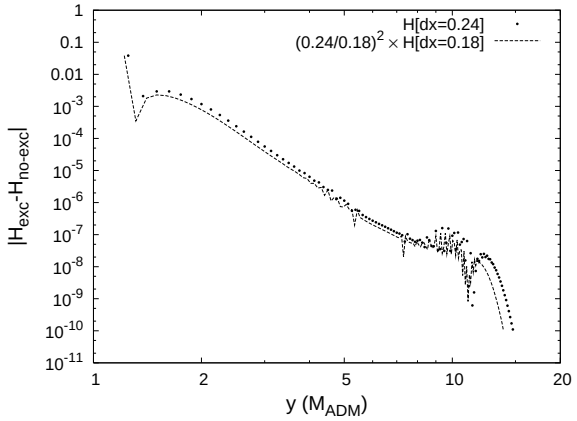

FIG. 3: Differences in the Hamiltonian constraints between the runs with and without excision $|H_{\rm exc} - H_{\rm no-exc}|$ at $T = 9.38M_{ADM}$ for the distorted black hole. The difference between the two cases converges away at second order.

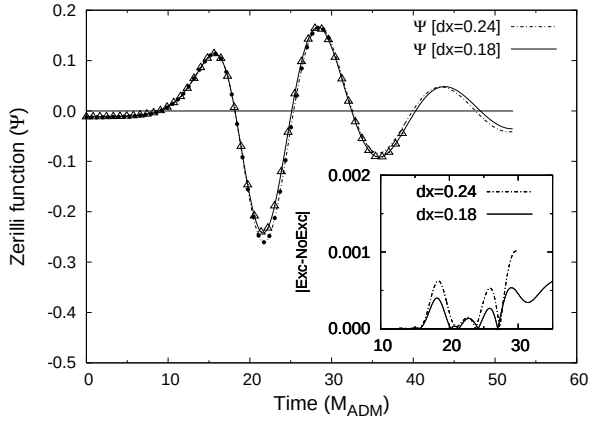

FIG. 5: Zerilli function ψ (ℓ = 2,m = 0 mode) calculated at $r = 13.5M_{ADM}$. The lines show the excision data and the points show the results of the simulations without excision. The inset shows the absolute value of the difference in the waveforms which decreases as the resolution is increased.

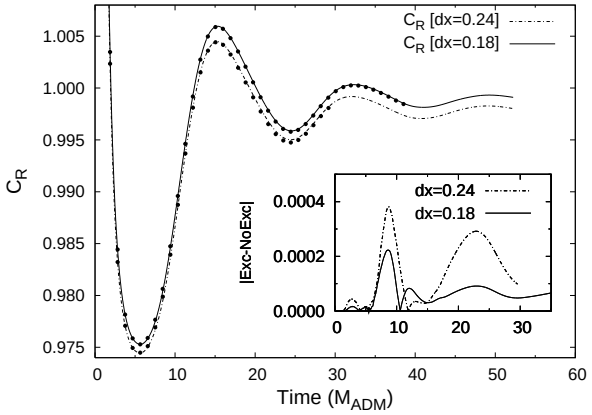

FIG. 4: Ratio C_r of the polar and equatorial circumference of the apparent horizon for two different resolutions of the distorted black hole simulation. The lines denote the excision data and the dots show the results of runs without excision. The inset shows the absolute value of the difference between the two cases.

function ψ (ℓ = 2, m = 0 mode). The figure shows excision data as lines and the results from simulations without excision as points. The absolute value of the difference between the waveforms is also shown in the inset. This difference is much smaller than the Zerilli function itself and decreases with resolution.

We also studied the effects of the size of the excision box for this model. One can expect that problems will occur if the excision box is made too large and in particular if it reaches outside of the black hole. In Fig. 6 we show the influence of differently sized excision boxes on the waveform. For these simulations the black hole is nearly spherical (see Fig. 4) with a mean coordinate radius of initially about 1 which then grows to about 2 during the first $5M_{ADM}$ of evolution. For comparison we have also used a cubical excision box which remained fixed throughout the evolution. The resolution used in these simulations was 0.18. We first plot the waveform of the lego excision simulation used above. Next we show waveforms for cubical excision regions where half the length of one side of the cube is 0.54, 0.90, 1.26 and 1.98, respectively. For the case with the smallest excision box the waveform remains essentially unaffected. However, once the excision region becomes larger and even extends outside of the initial apparent horizon a large effect on the waveform becomes visible. This demonstrates that excision must be done inside the horizon as one would expect. It also indicates that with techniques implemented here, a buffer zone of two to three points in the initial hole can be sufficient to accurately extract gravitational waves.

B. Results for Head-on Collision

As a second example we consider a binary BH head-on collision for Brill-Lindquist type data, starting from a close coordinate separation between punctures of 2.303. For this data set each individual BH has a mass parameter of $M_i = 0.5$ for a total ADM mass of $M_{ADM} = 1$ [56]. The initial data uses a "fish-eye" coordinate transformation to push the boundaries further out [33, 66]. We have performed runs using octant symmetry with central resolutions of 0.128, 0.064, and 0.032, on cubical grids with 96^3, 192^3 and 384^3 grid points respectively. Using the "fish-eye" parameters $a = 3$, $s = 1.2$ and $r_0 = 5.5$, in the notation of [33], places the coordinate boundaries at 12.288 and the physical boundaries at 25.862.

The evolution without excision is identical to the one shown in Figs. 11 and 12 of Ref. [33]. However, running the excision case with exactly the same parameters turned out to be impossible. The reason is that with the choice of damping coefficient η used in that reference

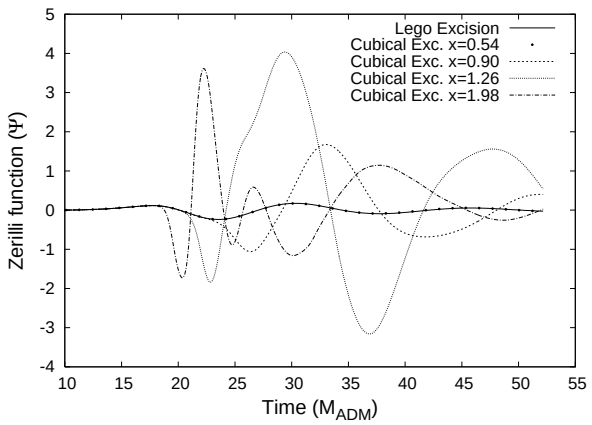

FIG. 6: Zerilli Function ψ for the distorted black hole calculated at $r = 15.3M_{ADM}$, using a resolution $dx = 0.18$ and different cubical excision box sizes. For the first two evolutions, the excised region is within the horizon and show essentially identical results for both the cubical and "lego" excision region. The other evolutions have at least a portion of the excision box extending outside the horizon, and thus do not represent true outflow boundaries. They show dramatic differences from the previous waveforms.

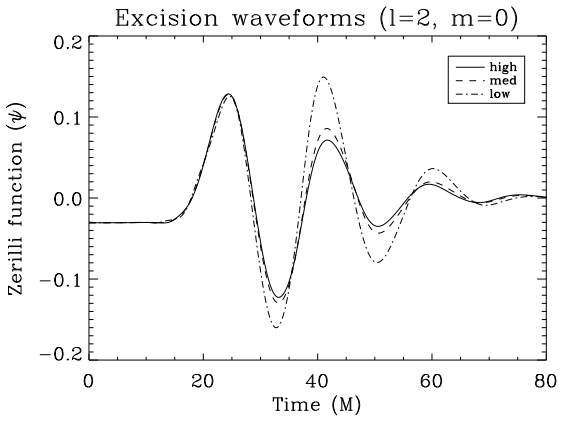

FIG. 7: Zerilli function ψ ($\ell = 2$, $m = 0$ mode) calculated at $r = 14.8M_{ADM}$ for the head-on collision using excision at resolutions 0.128 (low), 0.064 (med) and 0.032 (high).

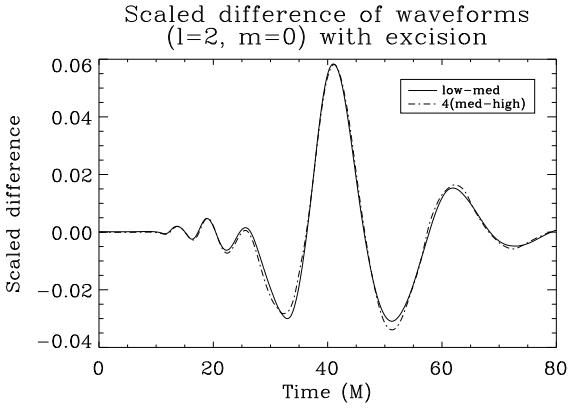

FIG. 8: Scaled difference of the Zerilli function ψ ($\ell = 2$, $m = 0$ mode) calculated at $r = 14.8M_{ADM}$ for the head-on collision using excision showing second order convergence.

for the Gamma driver shift condition, the lapse and shift turned out to be too dynamic at the excision boundary, causing the simulation to crash very early. We have found that this effect can be controlled by using a smooth spatially varying η-parameter. This was implemented using the conformal factor from the initial data

$$\Psi = 1 + \frac{M_1}{2r_1} + \frac{M_2}{2r_2}, \tag{3.1}$$

with M_1 and M_2 the mass parameters of the black holes (in this case $M_1 = M_2 = 0.5$) and r_1 and r_2 the coordinate distances to the two punctures. A smoothly varying η-parameter can then be constructed (this construction is of course not unique) as

$$\eta = \eta_{\rm punc} - \frac{\eta_{\rm punc} - \eta_\infty}{C\,(1 + (\Psi - 1)^2)}, \tag{3.2}$$

where $\eta_{\rm punc}$ is the value of η near the punctures, η_∞ is the value of η at infinity, and C is a parameter that controls the width of the transition region. Here we used $\eta_{\rm punc} = 5.6$, $\eta_\infty = 2.8$ and $C = 1$.

The resulting waveforms for the excision runs, using the above construction for η and the three different resolutions, can be seen in Fig. 7. These waveforms are second order convergent as can be seen from Fig. 8, where the difference between the low and medium resolution waveforms and four times the difference between the medium and high resolution waveforms are plotted together.

At all three resolutions we can see some differences in the waveforms between the runs with and without excisions. There are basically two reasons for this. The first is of course the presence of the excision boundary and the second is the slightly different gauge choices that were needed in each case in order to obtain long enough evolutions. However, as can be seen from Fig. 9, these differences converge away to second order with resolution (except for a small gauge effect which is visible in the initial part of the waveform).

For the above runs, we used an excision region which was 80% of the apparent horizon radius with minimum buffer size of (5,10,20) grid points for the three different resolutions. This was in order to ensure that we had a buffer zone large enough suppress inaccuracies at the excision boundary from propagating out of the hole, as well as to ensure that the apparent horizon can always be located, as this requires points on both sides of the surface.

We note that the runs performed with excision are more sensitive to gauge parameters than the evolutions without excision. This is essentially due to the fact that the shift can be used to control the rate of growth of

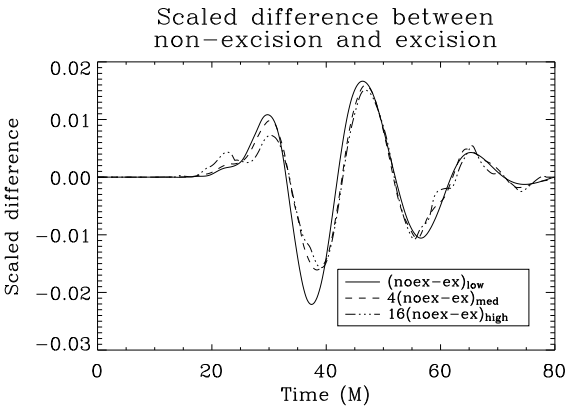

FIG. 9: Scaled difference in waveforms from evolutions with and without excision for the three different resolutions used in the head-on collision.

the horizon, and in some cases can even draw it inwards. For the excised runs, this means that the horizon can be brought too close to the excision boundary, allowing errors to "leak out". The shift parameters used in this paper allow a slightly faster growth of the horizon than those used in [33].

IV. CONCLUSIONS

We have proposed a sensitive test-bed for 3D black hole excision techniques in numerical relativity, whereby simulations with and without excision are carried out on identical initial data sets. A recently developed family of powerful gauge conditions now allows long evolutions of some black hole spacetimes without excision, making such a test-bed practical for the first time. Applying these ideas to our own methods, we demonstrated that our excision procedure is not only effective in improving the length of time that black holes can be evolved, but also that it preserves sensitive details of the physics that can be extracted. We carried out both distorted and binary black hole head-on collision simulations, both with and without excision. We used both the ratio of apparent horizon circumferences and the very sensitive indicator of extracted waveforms to compare physically important details of the simulations. In particular, the waveforms represent very small signals buried in the metric functions. The results are essentially identical, indicating that the excision boundary condition has preserved the accuracy of the runs.

The evolutions were carried out for cases of axisymmetric initial data, where for singularity avoiding slicing with an appropriate shift condition the evolution variables could be suitably controlled at the locations of the punctures. For more general situations it can be more difficult to maintain a regular evolution. In such situations, even for the puncture data discussed above, it is expected that excision would be necessary for a long-term evolution. However, the tests shown here have given us confidence that the excision methods which we are using are robust for reasonably complicated situations, and do not adversely affect the accuracy of evolutions.

Runs without excision form an important benchmark against which the effects of excision techniques can be analyzed. Evolutions of black hole spacetimes involve a patchwork of experimental techniques, all of which are needed to obtain long evolution times, but each of which carries with it complications that can affect the accuracy and stability of the simulation, both in isolation and in interaction with the entire system. Given this fact, the models considered above can form a particularly important test of the effects of applying an excision boundary condition.

The initial data sets we used here are readily available to anyone through the Cactus framework. This will make it possible for other groups to apply the same test-bed to their own evolution codes.

Acknowledgments

The lego excision code discussed in this paper was developed in collaboration with Erik Schnetter and Deirdre Shoemaker. Results for this paper were obtained using computing time allocations at the AEI, CCT, LRZ, NCSA, NERSC, PSC and RZG. We use Cactus and the `CactusEinstein` infrastructure with a number of locally developed thorns. This work was supported in part by NSF grants PHY-02-18750 and PHY-02-44788, by the DFG grant "SFB/Transregio 7: Gravitational Wave Astronomy", by DGAPA-UNAM grants IN112401 and IN122002, and by the EU Programme 'Improving the Human Research Potential and the Socio-Economic Knowledge Base' (Research Training Network Contract HPRN-CT-2000-00137).

[1] J. Thornburg, Master's thesis, University of British Columbia, Vancouver, British Columbia (1985).
[2] J. Thornburg, Class. Quantum Grav. **4**, 1119 (1987), URL `http://stacks.iop.org/0264-9381/4/1119`.
[3] J. Thornburg (1991), a talk given at CITA, Toronto, May, 1991.
[4] W. G. Unruh (1984).
[5] E. Seidel and W.-M. Suen, Phys. Rev. Lett. **69**, 1845 (1992).
[6] P. Anninos, K. Camarda, J. Massó, E. Seidel, W.-M. Suen, and J. Towns, Phys. Rev. D **52**, 2059 (1995).
[7] P. Anninos, G. Daues, J. Massó, E. Seidel, and W.-M.

Suen, Phys. Rev. D **51**, 5562 (1995).
[8] R. Marsa and M. W. Choptuik, Phys Rev D **54**, 4929 (1996).
[9] G. B. Cook, M. F. Huq, S. A. Klasky, M. A. Scheel, A. M. Abrahams, A. Anderson, P. Anninos, T. W. Baumgarte, N. Bishop, S. R. Brandt, et al., Phys. Rev. Lett **80**, 2512 (1998).
[10] R. Gómez, L. Lehner, R. Marsa, J. Winicour, A. M. Abrahams, A. Anderson, P. Anninos, T. W. Baumgarte, N. T. Bishop, S. R. Brandt, et al., Phys. Rev. Lett. **80**, 3915 (1998), gr-qc/9801069.
[11] P. Walker, Ph.D. thesis, University of Illinois at Urbana-Champaign, Urbana, Illinois (1998).
[12] S. Brandt, R. Correll, R. Gómez, M. F. Huq, P. Laguna, L. Lehner, P. Marronetti, R. A. Matzner, D. Neilsen, J. Pullin, et al., Phys. Rev. Lett. **85**, 5496 (2000).
[13] D. Shoemaker, K. L. Smith, U. Sperhake, P. Laguna, E. Schnetter, and D. Fiske, Class. Quantum Grav. **20**, 3729 (2003).
[14] B. Brügmann, Phys. Rev. D **54**, 7361 (1996), gr-qc/9608050.
[15] T. Nakamura, K. Oohara, and Y. Kojima, Progress of Theoretical Physics Supplement **90**, 1 (1987).
[16] M. Shibata and T. Nakamura, Phys. Rev. D **52**, 5428 (1995).
[17] T. W. Baumgarte and S. L. Shapiro, Phys. Rev. D **59**, 024007 (1999), gr-qc/9810065.
[18] M. Alcubierre, B. Brügmann, T. Dramlitsch, J. Font, P. Papadopoulos, E. Seidel, N. Stergioulas, and R. Takahashi, Phys. Rev. D **62**, 044034 (2000), gr-qc/0003071.
[19] M. Alcubierre, G. Allen, B. Brügmann, E. Seidel, and W.-M. Suen, Phys. Rev. D **62**, 124011 (2000), gr-qc/9908079.
[20] M. Alcubierre and B. Brügmann, Phys. Rev. D **63**, 104006 (2001), gr-qc/0008067.
[21] M. Alcubierre, B. Brügmann, D. Pollney, E. Seidel, and R. Takahashi, Phys. Rev. D **64**, 61501 (R) (2001), gr-qc/0104020.
[22] H.-J. Yo, T. Baumgarte, and S. Shapiro, Phys. Rev. D **64**, 124011 (2001).
[23] G. Calabrese, L. Lehner, D. Neilsen, J. Pullin, O. Reula, O. Sarbach, and M. Tiglio, Class. Quantum Grav. **20**, L245 (2003), gr-qc/0302072.
[24] G. Calabrese, L. Lehner, O. Reula, O. Sarbach, and M. Tiglio (2003), gr-qc/0308007.
[25] H.-J. Yo, T. Baumgarte, and S. Shapiro, Phys. Rev. D **66**, 084026 (2002).
[26] U. Sperhake, K. L. Smith, B. Kelly, P. Laguna, and D. Shoemaker, Phys. Rev. D **69**, 024012 (2003), gr-qc/0307015.
[27] L. E. Kidder, M. A. Scheel, S. A. Teukolsky, E. D. Carlson, and G. B. Cook, Phys. Rev. D **62**, 084032 (2000), gr-qc/0005056.
[28] L. E. Kidder, M. A. Scheel, and S. A. Teukolsky, Phys. Rev. D **64**, 064017 (2001), gr-qc/0105031.
[29] M. A. Scheel, L. E. Kidder, L. Lindblom, H. P. Pfeiffer, and S. A. Teukolsky, Phys. Rev. D **646**, 124005 (2002), gr-qc/0209115.
[30] G. Calabrese and D. Neilsen, Physical Review D **69**, 044020 (21 pages) (2004), gr-qc/0308008.
[31] J. Thornburg, Class. Quantum Grav. **21**, 3665 (2004), gr-qc/0404059, URL `http://stacks.iop.org/0264-9381/21/3665`.
[32] L. Lehner, O. Reula, and M. Tiglio (2004), in preparation.
[33] M. Alcubierre, B. Brügmann, P. Diener, M. Koppitz, D. Pollney, E. Seidel, and R. Takahashi, Phys. Rev. D **67**, 084023 (2003), gr-qc/0206072.
[34] B. Reimann (2004), gr-qc/0404118.
[35] K. Camarda and E. Seidel, Phys. Rev. D **57**, R3204 (1998), gr-qc/9709075.
[36] K. Camarda and E. Seidel, Phys. Rev. D **59**, 064019 (1999), gr-qc/9805099.
[37] G. Allen, K. Camarda, and E. Seidel (1998), gr-qc/9806036, submitted to Phys. Rev. D.
[38] G. Allen, K. Camarda, and E. Seidel (1998), gr-qc/9806014, submitted to Phys. Rev. D.
[39] P. Anninos, D. Hobill, E. Seidel, L. Smarr, and W.-M. Suen, Phys. Rev. Lett. **71**, 2851 (1993).
[40] P. Anninos, D. Hobill, E. Seidel, L. Smarr, and W.-M. Suen, Phys. Rev. D **52**, 2044 (1995).
[41] P. Anninos, R. H. Price, J. Pullin, E. Seidel, and W.-M. Suen, Phys. Rev. D **52**, 4462 (1995).
[42] T. W. Baumgarte, Phys. Rev. D **62**, 024018 (2000), gr-qc/0004050.
[43] W. Tichy, B. Brügmann, M. Campanelli, and P. Diener, Phys. Rev. D **67**, 064008 (2003), gr-qc/0207011.
[44] W. Tichy, B. Brügmann, and P. Laguna, Phys. Rev. D **68**, 064008 (2003), gr-qc/0306020.
[45] W. Tichy and B. Brügmann (2003), gr-qc/0307027.
[46] S. Brandt and B. Brügmann, Phys. Rev. Lett. **78**, 3606 (1997), gr-qc/9703066.
[47] L. Smarr and J. W. York, Jr., Phys. Rev. D **17**, 2529 (1978).
[48] D. Bernstein, D. Hobill, E. Seidel, and L. Smarr, Phys. Rev. D **50**, 3760 (1994).
[49] A. Abrahams, D. Bernstein, D. Hobill, E. Seidel, and L. Smarr, Phys. Rev. D **45**, 3544 (1992).
[50] P. Anninos, D. Bernstein, S. Brandt, Hobill, E. Seidel, and L. Smarr, Phys. Rev. D **50**, 3801 (1994).
[51] D. Bernstein, D. Hobill, E. Seidel, L. Smarr, and J. Towns, Phys. Rev. D **50**, 5000 (1994).
[52] S. Brandt and E. Seidel, Phys. Rev. D **52**, 870 (1995).
[53] S. Brandt and E. Seidel, Phys. Rev. D **54**, 1403 (1996).
[54] P. Anninos, D. Bernstein, S. Brandt, J. Libson, J. Massó, E. Seidel, L. Smarr, W.-M. Suen, and P. Walker, Phys. Rev. Lett. **74**, 630 (1995).
[55] S. Brandt, K. Camarda, E. Seidel, and R. Takahashi, Class. Quantum Grav. **20**, 1 (2003), gr-qc/0206070.
[56] D. Brill and R. Lindquist, Phys. Rev. **131**, 471 (1963).
[57] B. Brügmann, Int. J. Mod. Phys. D **8**, 85 (1999).
[58] K. Thorne, Phys. Rev. D (1999), gr-qc/9808024.
[59] M. Alcubierre, P. Diener, F. S. Guzmán, S. Hawley, M. Koppitz, D. Pollney, and E. Seidel, in preparation.
[60] M. Alcubierre, B. Brügmann, P. Diener, F. S. Guzmán, I. Hawke, S. Hawley, F. Herrmann, M. Koppitz, D. Pollney, E. Seidel, et al., in preparation.
[61] B. Brügmann, W. Tichy, and N. Jansen, Phys. Rev. Lett. **92**, 211101 (2004), gr-qc/0312112.
[62] M. D. Duez, P. Marronetti, S. L. Shapiro, and T. W. Baumgarte, Phys. Rev. D **67**, 024004 (2003), gr-qc/0209102.
[63] S. Brandt, K. Camarda, and E. Seidel, in *Proceedings of the 8th Marcel Grossmann Meeting on General Relativity*, edited by T. Piran (World Scientific, Singapore, 1999), pp. 741–743.
[64] E. Schnetter (2002), gr-qc/0206003.
[65] J. Thornburg, Class. Quantum Grav.

21, 743 (2004), gr-qc/0306056, URL http://stacks.iop.org/0264-9381/21/743.

[66] J. Baker, B. Brügmann, M. Campanelli, and C. O. Lousto, Class. Quantum Grav. **17**, L149 (2000), aEI-2000-015.

[67] Of course, with a poor choice of coordinates and gauge it may be the case that the stationarity takes on a very different form, however in practice we have found that the gauge choices which we apply do drive the system to a state in which the time derivatives tend to zero [33]